v_1, v_2	=	molar volume of components 1 and 2 in liquid	$[m^3 \cdot mol^{-1}]$
x_1, x_2	=	mole fraction of components 1 and in liquid	[—]
δ	=	hole diameter in gas distributor	[m]
ε_G	=	gas holdup	[—]
ε_L	=	liquid holdup	[—]
ε_S	=	solid holdup	[—]
μ_L	=	liquid viscosity	[Pa·s]
ν	=	total number of moles of ions per mole of electrolyte or 1 for non-electrolyte	[—]
ρ_L	=	liquid density	$[kg \cdot m^{-3}]$
ρ_S	=	solid density	$[kg \cdot m^{-3}]$
σ_L	=	liquid surface tension	$[N \cdot m^{-1}]$

〈Subscripts〉

est	=	estimated value
obs	=	observed value
0	=	without solid particles

Literature Cited

1) Akita, K. and F. Yoshida: *Ind. Eng. Chem., Process Des. Dev.*, **12**, 76 (1973).
2) Himmelblau, D. M.: "Process Analysis by Statistical Methods," p. 178, John Wiley & Sons (1970).
3) Koide, K., K. Horibe, H. Kawabata and S. Ito: *J. Chem. Eng. Japan*, **17**, 368 (1984).
4) Koide, K., K. Horibe, H. Kitaguchi and N. Suzuki: *J. Chem. Eng. Japan*, **17**, 547 (1984).
5) Koide, K., K. Kurematsu, S. Iwamoto, Y. Iwata and K. Horibe: *J. Chem. Eng. Japan*, **16**, 413 (1983).
6) Koide, K., H. Sato and S. Iwamoto: *J. Chem. Eng. Japan*, **16**, 407 (1983).
7) Koide, K., A. Takazawa, M. Kōmura and H. Matsunaga: *J. Chem. Eng. Japan*, **17**, 459 (1984).
8) Lamont, A. G. W.: *Can. J. Chem. Eng.*, **31**, 153 (1958).
9) Marrucci, G.: *Chem. Eng. Sci.*, **24**, 975 (1969).
10) Muroyama, K., A. Yasunishi and Y. Mitani: Proceedings of the Third Pacific Chem. Eng. Congress, **1**, 303 (1983).

(Presented in part at the 49th Annual Meeting of The Society of Chemical Engineers, Japan at Nagoya, April 3, 1984.)

LATERAL SOLID MIXING IN THE FLUIDIZED BED WITH MULTI-TUBES INTERNALS

KUNIO KATO, YUKINORI SATO, DAISUKE TANEDA AND TAKETOSHI SUGAWA

Department of Chemical Engineering, Gunma University, Kiryu 376

Key Words: Fluidized Bed, Solid Mixing, Diffusion Model, Lateral Dispersion Coefficient, Internals, Residence Time Distribution

The lateral mixing of fluidized particles in a fluidized bed with vertical or horizontal multi-tube internals was investigated by the unsteady state behaviour of tracer particles. The behaviour of the tracer particles is analyzed by a one-dimensional diffusion model. The tracer particles were activated alumina on which zinc acetate was adsorbed. The lateral diffusion coefficient of the particles was strongly affected by the hydraulic diameter of the internals, the gas velocity and the minimum fluidized gas velocity of the particles.

Empirical equations for the lateral diffusion coefficient of the particles in a fluidized bed with vertical or horizontal multi-tube internals were obtained.

The lateral diffusion coefficient of solid particles in an ordinary fluidized bed was correlated by an empirical equation. Thermal diffusivity obtained from lateral thermal conductivity in the fluidized bed with multi-tube internals agreed with the lateral diffusion coefficient at the same fluidized conditions.

Introduction

Fluidized beds are used for drying of particles and as a solid-gas reactor such as coal combustor, regenerator of spent activated carbon or roaster of zinc blende. To analyze these processes it is very important to estimate the residence time distribution of fluidized particles in the bed.

Received October 25, 1984. Correspondence concerning this article should be addressed to K. Kato. Y. Sato is now with Isobe Works, Shinetsu Chemical Co., Ltd., Annaka 379-01. D. Taneda is now with Ōarai Nuclear Power Engineering Developing Center, JGC Co., Ltd., Ōarai, 311-13. T. Sugawa is now with Ryowa Air-Conditioning Co., Ltd.

The behaviour of fluidized particles is usually analyzed by the following models: turnover rate model,[11] diffusion model[2,3,5,6,10] and two-phase model.[1] However, the relationship between the model parameter of these models and the operating conditions of fluidized beds is not yet established.

Generally the mixing of fluidized particles in an ordinary fluidized bed is very fast, and suitable internals in the bed are quite effective in controlling the mixing rate.

Gabor[4] investigated the lateral solid mixing in a

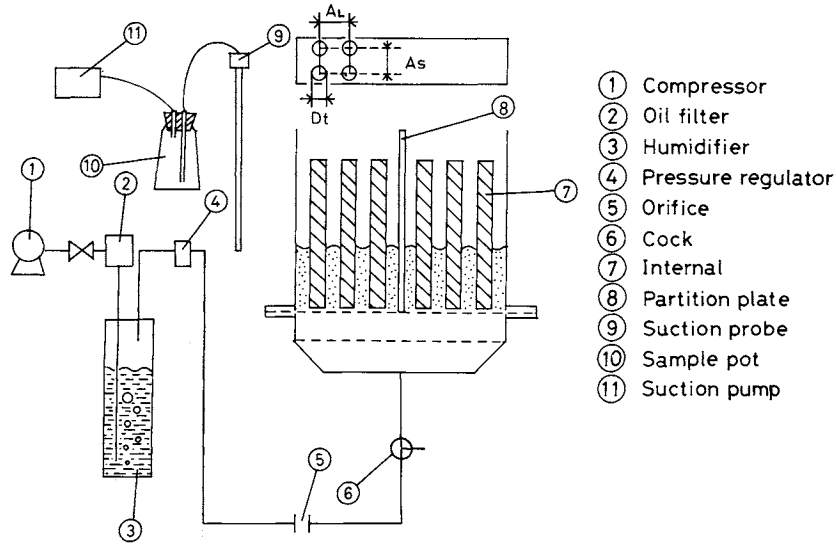

Fig. 1. Experimental apparatus.

packed fluidized bed with spherical packings and analyzed it by a diffusion model. An empirical equation for the lateral dispersion coefficient was obtained. Kato *et al.*[7] obtained an empirical equation for the lateral dispersion coefficient of solid particles in a packed fluidized bed with screen packings.

When a fluidized bed is used for an exothermic reaction with a large heat of reaction, cooling tubes are immersed in the bed to remove heat from the bed.

In the present work the lateral solid mixing in a fluidized bed with vertical or horizontal multi-tube internals was investigated by using tracer particles. The tracer particles were activated alumina particles on which zinc acetate was adsorbed. The lateral mixing characteristics are analyzed by a diffusion model. The effects of superficial gas velocity, internals and minimum fluidizing gas velocity upon the lateral dispersion coefficient of the particles are investigated.

1. Experimental Apparatus and Procedure

The experimental apparatus is shown in **Fig. 1**. The fluidized bed consisted of a rectangular column made of acrylic resin, 50 cm wide, 20 cm long and 70 cm high. A perforated plate made of acrylic resin of 5 mm thickness, 2 mm pore size, and 2.0% open area was used as the gas distributor.

To prevent the adhesion of particles to the bed wall

Table 1. Properties of fluidized particles

D_p [cm]	Umf [cm/s]	ϕ_s [—]	ε_{mf} [—]
0.0394	3.5	1.0	0.45
0.0477	5.0	1.0	0.45
0.0511	7.3	1.0	0.45
0.0920	20.0	1.0	0.45
0.1073	27.0	1.0	0.45

Table 2. Size and arrangement of vertical multi-tube internals

D_t [cm]	A_s [cm]	A_L [cm]	$m1$ [—]	$m2$ [—]	D_e [cm]
3.2	4.0	4.0	5	12	2.7
3.2	5.0	5.0	4	10	5.0
3.2	4.0	8.0	5	6	6.8
3.2	8.0	8.0	3	6	10.6

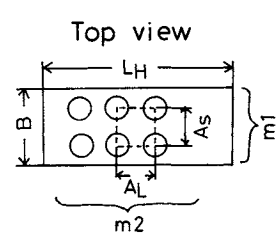

Table 3. Size and arrangement of horizontal multi-tube internals

D_t [cm]	S_T [cm]	S_L [cm]	$m2$ [—]	$m3$ [—]	D_e [cm]
1.8	2.5	2.5	18	4	2.6
1.8	5.0	2.5	10	4	7.0
1.8	5.0	5.0	10	2	15.9

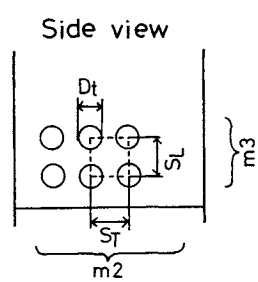

by static electricity, the inside wall of the bed was coated with Teflon. Air was passed through a water bath and was humidified and then supplied to the bed. Particles of activated alumina were used as fluidized particles. Properties of the fluidized particles are shown in **Table 1**. The size and arrangement of vertical and horizontal multi-tube internals are respectively shown in **Tables 2** and **3**. The hydraulic diameters of vertical and horizontal multi-tube internals in the bed are respectively calculated from Eqs. (1) and (2).

$$De=\frac{4\left(L_H\cdot B-m_1\cdot m_2\pi\frac{Dt^2}{4}\right)}{2(L_H+B)+m_1\cdot m_2\pi D_t} \tag{1}$$

$$De=\frac{4(S_L\cdot S_T-\pi Dt^2/4)}{\pi D_t} \tag{2}$$

The tracer particles were made as follows. Six liters of activated alumina were put into 8 liters of water containing 268 g zinc acetate and was mixed for an hour while zinc acetate was adsorbed on the particles. The particles were filtered out and dried at 353 K.

The experimental procedure was as follows. The partition plate was placed vertically in the center of the bed. The activated alumina particles were put in one side, the tracer particles in the other. After fluidizing the particles for a few minutes at constant gas velocity, the partition plate was suddenly pulled up and the particles were then fluidized for a certain period at the constant gas velocity. The fluidization was suddenly stopped by quickly shutting the ball valve. The sample particles were taken from the bed by using an 8 mm i.d. suction probe at several points. To obtain the concentration distribution of the tracer particles in the bed, the concentration of zinc acetate in the sample particles was measured.

Before this experiment the lateral mixing of the particles was visually observed by means of colored tracer particles.

2. Experimental Results

It seems that the diffusion model is suitable for the analysis of the lateral mixing of particles in a fluidized bed with multi-tube internals. From the material balance of tracer particles in the lateral direction the following equation is obtained.

$$\frac{\partial C}{\partial\theta}=Dsr\left(\frac{\partial^2 C}{\partial X^2}\right) \tag{3}$$

The initial and boundary conditions

I.C. $\theta=0 \quad 0\leqq X\leqq L_1\,; \quad C=1$

$\theta=0 \quad L_1\leqq X\leqq L_H\,, \quad C=0$

B.C. $X=0\,, \quad X=L_H\,; \quad \dfrac{\partial C}{\partial x}=0$

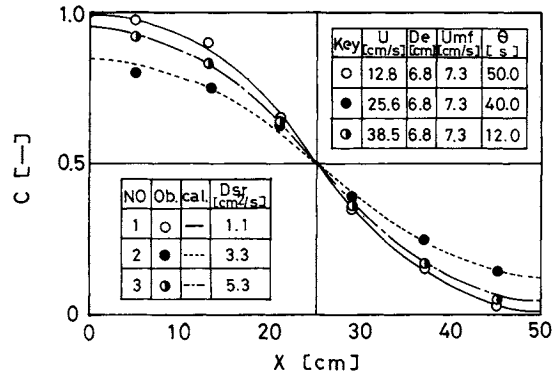

Fig. 2. Concentration distribution of tracer particles.

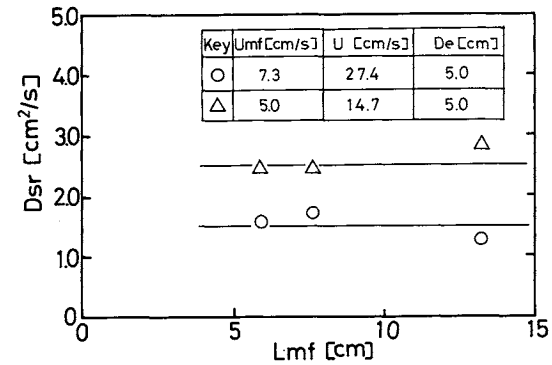

Fig. 3. Effect of bed height upon lateral diffusion coefficient.

An analytical solution of Eq. (3) with the above conditions becomes:

$$C=\frac{L_1}{L_H}+\frac{2}{\pi}\sum_{n=1}^{\infty}\frac{1}{n}\sin\frac{n\pi L_1}{L_H}\cdot\cos\frac{n\pi X}{L_H}\exp\left(-\frac{n^2\pi^2}{L_H^2}Dsr\theta\right) \tag{4}$$

The lateral diffusion coefficient of the particles *Dsr* is obtained by comparing the measured concentration distribution with the calculated concentration distribution by Eq. (4).

Figure 2 shows the lateral concentration distribution of tracer particles with gas velocity as a parameter. In this figure, each point is an experimental datum and each line is the value calculated from Eq. (4) for the case where the most suitable diffusion coefficient is used. From Fig. 2, experimental data well fit the calculated concentration distribution. It is considered that the lateral concentration distribution of tracer particles can be well expressed by the diffusion model.

Figure 3 shows the effect of the bed height at the minimum fluidizing gas velocity upon the lateral diffusion coefficient *Drs* in the case of vertical multi-tube internals. From Fig. 3 *Dsr* is not dependent upon *Lmf*. This result is quite different from the result obtained by Hirama *et al.*[6] in an ordinary fluidized bed. It seems that the mixing of particles is not

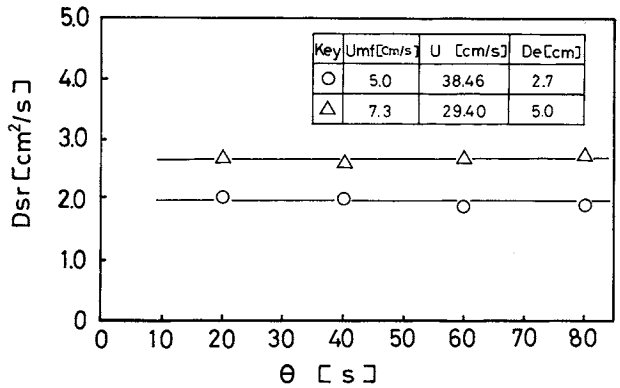

Fig. 4. Effect of elapsed time upon lateral diffusion coefficient.

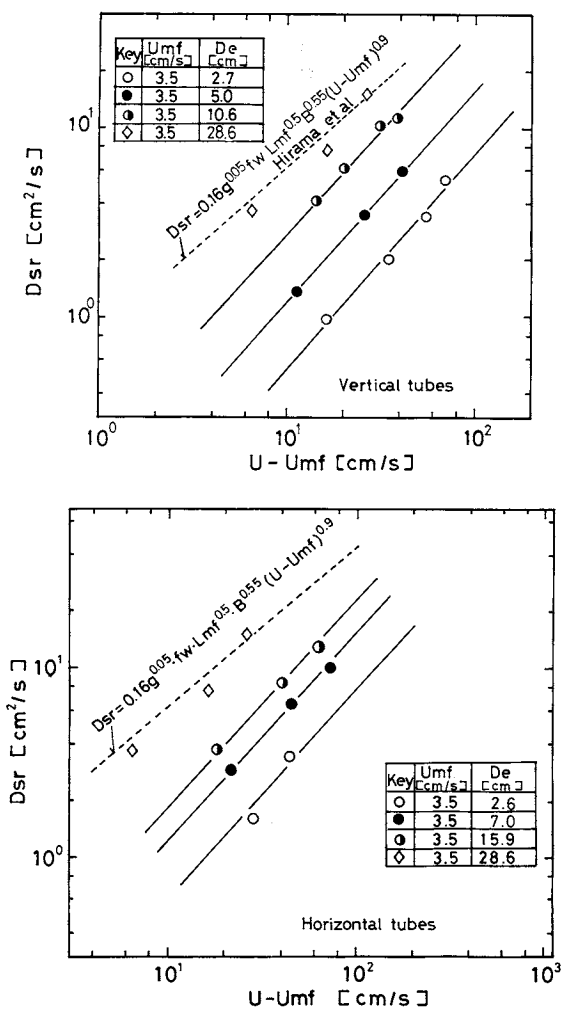

Fig. 5. Relation between *Dsr* and $U-Umf$.

affected by *Lmf* because the internals control the growth of gas bubbles.

Figure 4 shows the effect of the elapsed time θ upon *Dsr*. From Fig. 4, *Dsr* is not affected by θ and *Dsr* is not affected by elapsed time. From this figure, it can be confirmed that the lateral concentration distribution is well expressed by the diffusion model.

Figures 5-a and **5-b**, respectively, show the relation between $U-Umf$ and the lateral diffusion coefficient

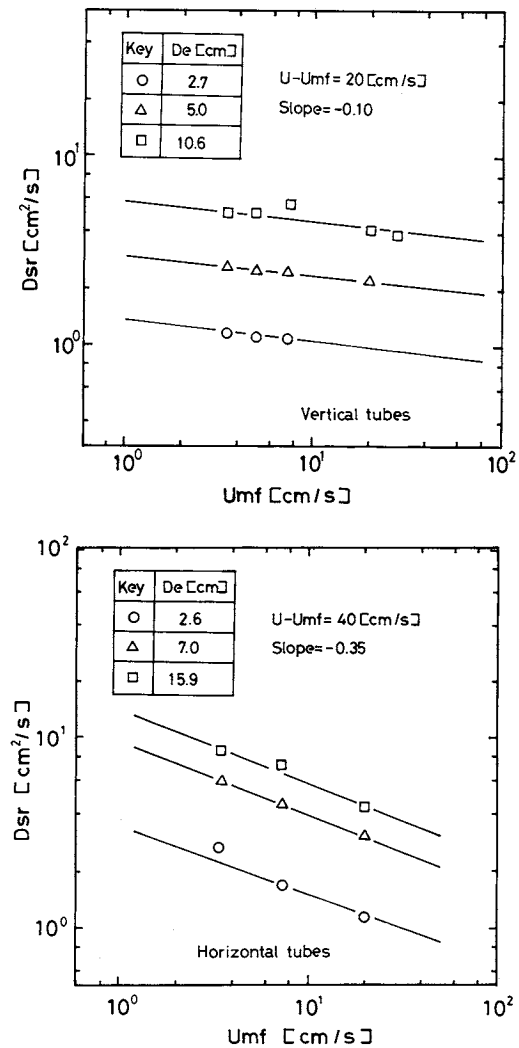

Fig. 6. Relation between *Dsr* and *Umf*.

Dsr with the hydraulic diameter *De* as a parameter in the case of vertical multi-tube internals and horizontal multi-tube internals. As gas velocity increases, *Dsr* increases. *Dsr* measured in an ordinary fluidized bed is also shown in Figs. 5-a and 5-b. These data are agree well with the empirical equation of Hirama *et al.*[6] *Drs* in the fluidized bed with internals is much smaller than that in an ordinary fluidized bed.

Figures 6-a and **6-b**, respectively, show the relation between the minimum fluidizing gas velocity *Umf* and the lateral diffusion coefficient *Dsr* with the hydraulic diameter *De* as a parameter in the case of vertical tubes and horizontal tubes. As the minimum gas velocity increases, *Dsr* decreases.

Figures 7-a and **7-b**, respectively, show the relation between the hydraulic diameter *De* and the lateral diffusion coefficient *Dsr* with the minimum fluidizing gas velocity *Umf* as a parameter in the case of vertical tubes and horizontal tubes. As the hydraulic diameter increases, *Dsr* increases.

In this experiment the effect of internals upon the solid mixing characteristics is expressed by the hy-

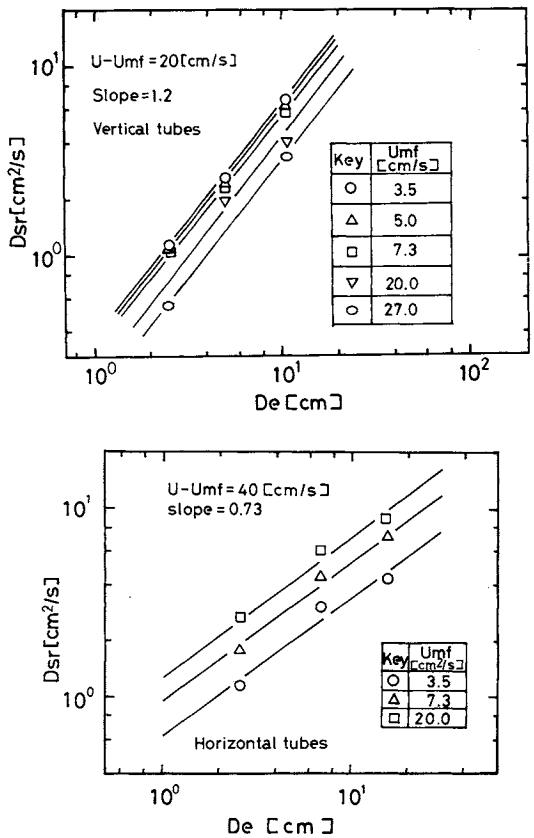

Fig. 7. Relation between *Dsr* and *De*.

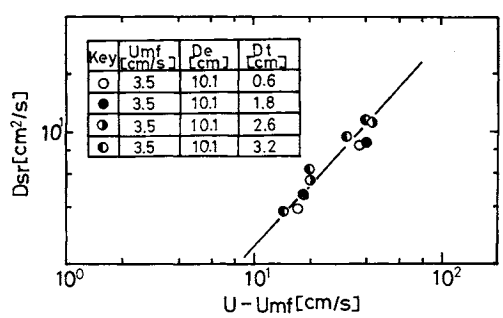

Fig. 8. Relation between *Dsr* and $U-Umf$.

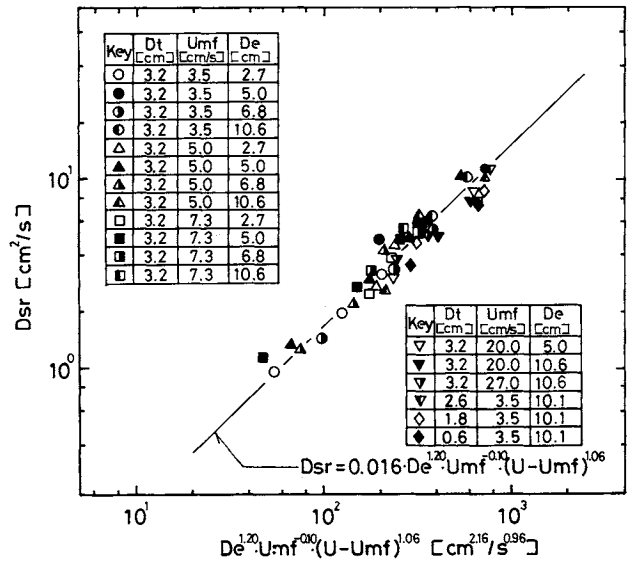

Fig. 9-a. Relation between *Dsr* and $De^{1.20}\cdot Umf^{-0.10}\cdot(U-Umf)^{1.06}$.

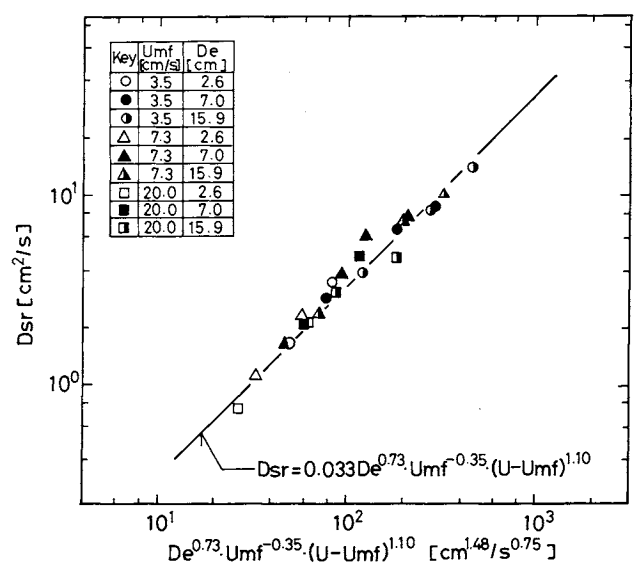

Fig. 9-b. Relation between *Dsr* and $De^{0.73}\cdot Umf^{-0.35}\cdot(U-Umf)^{1.10}$.

draulic diameter. **Figure 8** shows the effect of tube diameter upon *Dsr* at constant hydraulic diameter. From Fig. 8, the lateral diffusion coefficient *Dsr* is not affected by D_T at constant hydraulic diameter.

From Figs. 5, 6 and 7, *Dsr* is proportional to $(U-Umf)^{1.06}$, $Umf^{-0.10}$ and $De^{1.2}$ in the fluidized bed with vertical tube internals, and *Dsr* is proportional to $(U-Umf)^{1.10}$, $Umf^{-0.35}$ and $De^{0.73}$ in the fluidized bed with horizontal tube internals. **Figures 9-a** shows the relationship between *Dsr* and $De^{1.20}\cdot Umf^{-0.10}\cdot(U-Umf)^{1.06}$ in the case of vertical multi-tube internals. From Fig. 9-a, the following empirical equation is obtained for the fluidized bed with vertical tubes:

$$Dsr=0.016De^{1.20}\cdot Umf^{-0.10}\cdot(U-Umf)^{1.06} \quad (5)$$

Figure 9-b shows the relationship between *Dsr* and $De^{0.73}\cdot Umf^{-0.35}\cdot(U-Umf)^{1.10}$ in the case of horizontal multi-tube internals. From Fig. 9-b the following empirical equation is obtained for the fluidized bed with horizontal tube internals:

$$Dsr=0.033De^{0.73}\cdot Umf^{-0.35}\cdot(U-Umf)^{1.10} \quad (6)$$

The applicable ranges are as follows: *De*, 2.0–30.0 [cm]; *Umf*, 1–50 [cm/s]; *U*, 2–150 [cm/s].

3. Discussion

When gas velocity increases, the bubble frequency increases, particle movement becomes vigorous and *Dsr* increases, as shown in Fig. 5.

When the hydraulic diameter *De* increases, *Dsr* increases as shown in Fig. 7. When the hydraulic diameter decreases, the distance between tubes de-

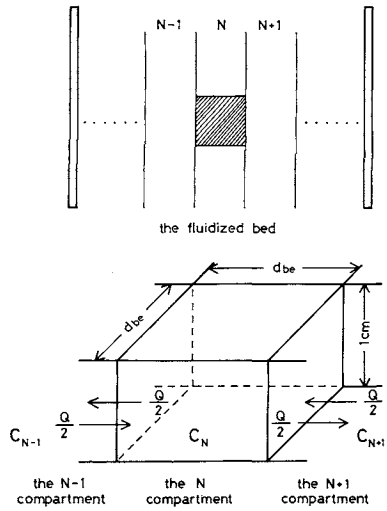

Fig. 10. Lateral solid mixing mechanism in the fluidized bed with multi-tube internals.

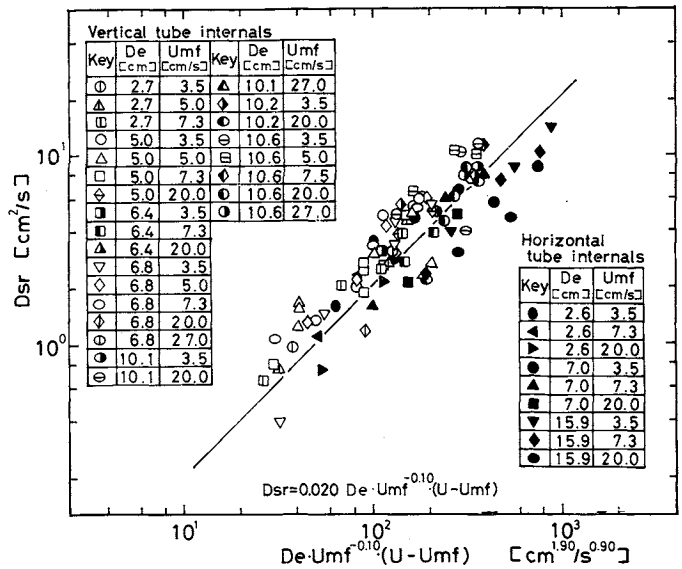

Fig. 11. Relation between Dsr and $De \cdot Umf^{-0.10} \cdot (U-Umf)$.

creases, the average bubble size in the bed becomes small and the scale of solid mixing becomes small.

From the information mentioned above, it is considered that the lateral diffusion coefficient is strongly affected by $U-Umf$ and De.

To analyze the lateral solid mixing in the bed, the following assumptions are made.

1) As the axial solid mixing rate is much larger than the lateral solid mixing rate, the concentration of the tracer particles is uniform in the axial direction.

2) The lateral transfer of particles in the bed is due to the movement of gas bubbles.

3) The effective bubble diameter d_{be} is assumed to be constant in the fluidized bed with tube internals.

4) The scale of lateral solid mixing is the same order of magnitude as the effective bubble diameter. When the bubbles rise in the fluidized bed, the amount of particles moved in a lateral direction per unit height is expressed by Q.

5) The concentrations of tracer particles in the $N-1$ compartment, the N compartment and the $N+1$ compartment are respectively expressed by C_{N-1}, C_N, C_{N+1}.

Now, mass balance of tracer particles per unit vertical height in the Nth compartment in **Fig. 10** gives the following equation.

$$1 \cdot d_{be} \cdot d_{be} \frac{\Delta C}{\Delta \theta} = \frac{Q}{2}(C_{N-1} + C_{N+1} - 2C_N) \qquad (7)$$

6) When a single bubble passes through the compartment, the amount of particles moved in the lateral direction is proportional to the surface area of the bubble.

$$q = \beta \cdot \pi \cdot d_{be}^2$$

The frequency of bubbles passing through the Nth compartment is:

$$M = \frac{d_{be}^2 (U - U_{mf})}{\frac{\pi}{6} d_{be}^3}$$

$$Q = q \cdot M = 6 \cdot \beta \cdot d_{be}(U - Umf) \qquad (8)$$

From Eqs. (7) and (8),

$$\frac{\Delta C}{\Delta \theta} = 3\beta d_{be}(U - Umf) \frac{(C_{N+1} - C_N) - (C_N - C_{N+1})}{d_{be}^2} \qquad (9)$$

To compare Eq. (3) with Eq. (9), Dsr corresponds to $3 \cdot \beta \cdot d_{be} \cdot (U - Umf)$. Since the bubble diameter is controlled by the internals, the effective bubble diameter in the bed will be approximately equal to the hydraulic diameter, that is, $d_{be} = De$

$$Dsr = 3\beta \cdot De \cdot (U - Umf) \qquad (10)$$

From Eq. (10), the lateral diffusion coefficient Dsr in the fluidized bed with tube internals is proportional to De and $U-Umf$. From Fig. 6 all experimental data can be approximately correlated between Dsr and $De \cdot Umf^{-0.10} \cdot (U-Umf)$. **Figure 11** shows the relationship between Dsr and $De \cdot Umf^{-0.10} \cdot (U-Umf)$. From this figure, the following empirical equation for the fluidized bed with vertical and horizontal tube internals is obtained.

$$Dsr = 0.020 De \cdot Umf^{-0.10}(U - Umf) \qquad (11)$$

De is calculated from the bed diameter or bed size of the ordinary fluidized bed by the same definition as that for the fluidized bed with internals. **Figure 12** shows the relationship between the lateral diffusion coefficient in an ordinary fluidized bed and $De^{1.20} \cdot Umf^{-0.10} \cdot (U-Umf)^{1.06}$. From Fig. 12 the lateral diffusion coefficient in an ordinary fluidized bed can be approximately correlated by the empirical equation for the fluidized bed with vertical tube

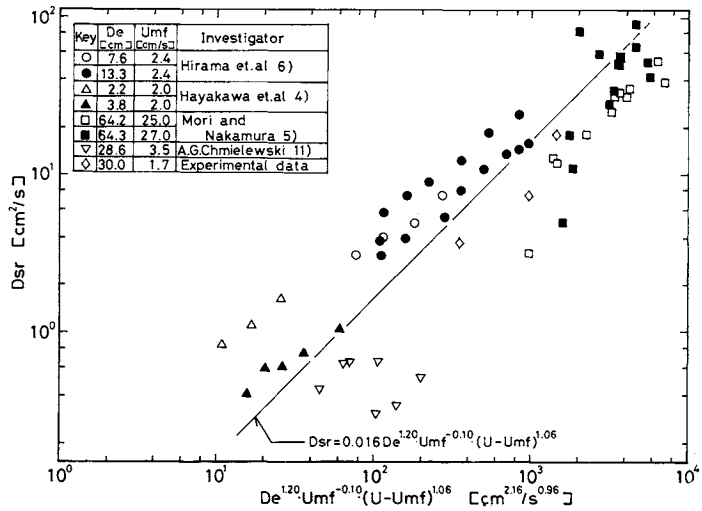

Fig. 12. Correlation of lateral diffusion data in the fluidized bed with no internals by empirical equation.

internals.

The mixing of fluidized particles may be the main factor in the lateral effective thermal conductivity in the bed.

Figure 13 compares the calculated *Dsr* from Eq. (11) with thermal diffusivity obtained by Kato *et al.*[8,9] Thermal diffusivity is given by the following equation.

$$\alpha = \frac{Ke}{C_{ps} \cdot \rho_B} \tag{12}$$

From Fig. 13, the thermal diffusivity obtained from the lateral thermal conductivity agrees approximately with the lateral diffusion coefficient at the same fluidized conditions.

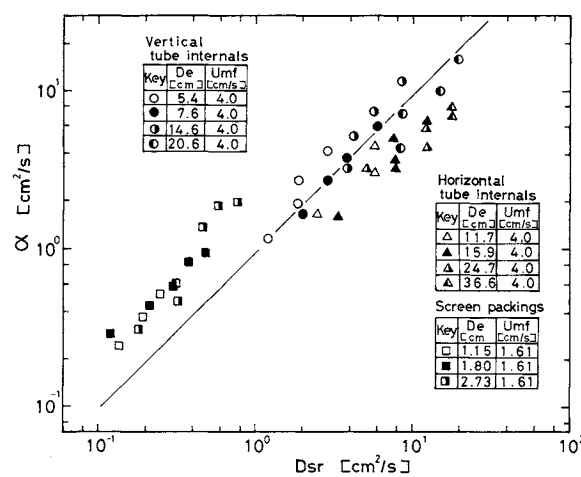

Fig. 13. Comparison of α calculated from lateral effective thermal conductivity with *Dsr* from Eq. (11).

4. Conclusion

1) The lateral solid mixing characteristics in the fluidized bed with tube internals is expressed by the diffusion model.

2) The lateral diffusion coefficient of particles in the fluidized bed with tube internals is strongly affected by the hydraulic diameter of tube internals and $U-Umf$. The following empirical equations are obtained:

For the fluidized bed with vertical tube internals

$$Dsr = 0.016 De^{1.20} \cdot Umf^{-0.10} \cdot (U-Umf)^{1.06}$$

For the fluidized bed with horizontal tube internals

$$Dsr = 0.033 De^{0.73} \cdot Umf^{-0.35} (U-Umf)^{1.10}$$

The applicable ranges are as follows: *De*, 2.0–30.0 [cm]; *Umf*, 1–50 [cm/s]; *U*, 2–150 [cm/s].

3) A simple model to explain the lateral solid mixing in the fluidized bed with tube internals is proposed. It can be well explained from this model that *Dsr* is strongly affected by *De* and $U-Umf$.

4) If *De* is equal to bed diameter or bed size, the lateral diffusion coefficient in the ordinary fluidized bed can be approximately correlated by the empirical equation obtained by this investigation.

5) The thermal diffusivity obtained from the lateral thermal conductivity agrees approximately with the lateral diffusion coefficient at the same fluidizing conditions.

Acknowledgment

This work was supported in part by a Grant-in-Aid by the Japan Securities Scholarship Foundation. The authors express their thanks for this financial support.

Nomenclature

A_L	=	tube interval in lateral direction	[cm]
As	=	tube interval in direction of width	[cm]
B	=	width of fluidized bed	[cm]
C	=	dimensionless concentration of tracer particles	[—]
C_N	=	concentration of tracer particles in compartment N	[g-tracer/cm³]

C_{ps}	=	heat capacity of fluidized particles	[kJ/kg K]
De	=	hydraulic diameter	[cm]
D_p	=	particle diameter	[cm]
Dsr	=	lateral diffusion coefficient	[cm^2/s]
D_t	=	tube diameter	[cm]
d_{be}	=	effective diameter of bubble	[cm]
Ke	=	lateral effective thermal conductivity	[KJ/kg·m·K]
L_f	=	bed height at fluidized gas velocity	[cm]
L_H	=	lateral length of fluidized bed	[cm]
Lmf	=	bed height at minimum fluidized gas velocity	[cm]
L_1	=	lateral length in fluidized bed from left wall to partition plate	[cm]
$m1$	=	number of tube in wide direction	[—]
$m2$	=	number of tube in lateral direction	[—]
$m3$	=	number of tube in axial direction	[—]
Q	=	amount of particles moved in lateral direction per unit height	[cm^3/s]
q	=	amount of particles moved in lateral direction when a single bubble passes through the compartment	[cm^3]
U	=	fluidized gas velocity	[cm/s]
Umf	=	minimum fluidized gas velocity	[cm/s]
X	=	lateral distance from left wall of fluidized bed	[cm]
α	=	thermal diffusivity	[cm^2/s]
β	=	proportional constant	[cm/s]
ε_f	=	void fraction at fluidized conditions	[—]
ε_{mf}	=	void fraction at minimum fluidizing conditions	[—]
ρ_b	=	bulk density of fluidized particles	[g/cm^3]
ρ_p	=	density of particles	[g/cm^3]
θ	=	elapsed time	[s]
ϕ_s	=	sphericity of fluidized particle	[—]

Literature Cited

1) Babu, S. P., S. Leipziger, B. S. Lee and S. A. Weil: *AIChE Symp. Ser.*, **69**, 49 (1973).
2) Brotz, W.: *Chem. Ing. Tech.*, **28**, 165 (1956).
3) Chmielewski, G. A. and A. Selecki: *Inzynieria Chemiczna*, **3**, 549 (1977).
4) Gabor, J. D.: *AIChE J.*, **10**, 345 (1964).
5) Hayakawa, T. and W. Graham: *Can. J. Chem. Eng.*, **41**, 99 (1964).
6) Hirama, T., M. Ishida and T. Shirai: *Kagaku Kogaku Ronbunshu*, **1**, 272 (1975).
7) Kato, K., D. Taneda, Y. Sato and M. Maa: *J. Chem. Eng. Japan*, **17**, 78 (1984).
8) Kato, K., T. Takahashi, K. Komagata, Y. Ōtubo and T. Sasaki: Conference papers, China-Japan Fluidized Bed Symposium, p. 214.
9) Kato, K., T. Takahashi, K. Komagata, Y. Ōtubo and T. Sasaki: *J. Chem. Eng. Japan*, **15**, 39 (1982).
10) Mori, Y. and K. Nakamura: *Kagaku Kogaku Ronbunshu*, **29**, 868 (1965).
11) Talmor, E. and R. F. Benenati: *AIChE J.*, **9**, 536 (1963).

EFFECT OF SYSTEM AGING ON RELEASE PROFILE OF RESERVOIR-TYPE DRUG DELIVERY SYSTEM

KAKUJI TOJO, YING SUN AND YIE W. CHIEN

Controlled Drug Delivery Research Center, Rutgers University College of Pharmacy, Piscataway, New Jersey 08854

Key Words: Controlled Release, Membrane Transport, Drug Delivery System, Time-Lag, Bursting, Solicone Membrane, 17α-Methyltestosterone

Introduction

The transient characteristics of drug release from a reservoir-type drug delivery system is of importance in the optimum design of controlled-release products. If the drug delivery system is applied shortly after manufacturing, a significant time-lag may be observed before constant release is achieved because the drug molecules do not exist in the fresh rate-controlling membrane initially. When the delivery system has been stored for a while, the drug molecules gradually penetrate into the rate-controlling membrane. And, finally, after a certain period of storage, the drug delivery system will show a typical bursting release due to the release of drug molecules already saturated in the membrane into its surroundings.[5] Since the time-dependent release rate observed initially for the reservoir-type drug delivery system is markedly influenced by the concentration profile of a drug inside the rate-controlling membrane prior to the onset of release, the aging (storage or history) of the drug delivery system should be carefully controlled. With an appropriate aging period, both the time-lag and bursting release could be minimized.

Received August 14, 1984. Correspondence concerning this article should be addressed to K. Tojo.